SLAC-PUB-7368
October 1997

Active High-Power RF Pulse Compression Using Optically Switched Resonant Delay Lines

Sami G. Tantawi[*], Ronald D. Ruth[*], Arnold E. Vlieks[*],
and Max Zolotorev[†]

[†]*Lawrence Berkeley Laboratory*
Berkeley, California, USA 94720

and

[*]*Stanford Linear Accelerator Center*
Stanford University
Stanford, California USA 94309

Presented at the the Seventh Workshop on Advanced Accelerator Concepts,
Lake Tahoe, CA, October 13-19, 1996

Work supported by Department of Energy contract DE–AC03–76SF00515.

Active High Power RF Pulse Compression Using Optically Switched Resonant Delay Lines

Sami G. Tantawi[*] , Ronald D. Ruth, Arnold E. Vlieks, and Max Zolotorev[**]

Stanford Linear Accelerator Center, Stanford University, Stanford, CA 94309, USA
[**] Lawrence Berkeley Lab. Berkeley, CA., USA

We present the design and a proof of principle experimental results of an optically controlled high power rf pulse compression system. The design should, in principle, handle few hundreds of Megawatts of power at X-band. The system is based on the switched resonant delay line theory [1]. It employs resonant delay lines as a means of storing rf energy. The coupling to the lines is optimized for maximum energy storage during the charging phase. To discharge the lines, a high power microwave switch increases the coupling to the lines just before the start of the output pulse. The high power microwave switch, required for this system, is realized using optical excitation of an electron-hole plasma layer on the surface of a pure silicon wafer. The switch is designed to operate in the TE_{01} mode in a circular waveguide to avoid the edge effects present at the interface between the silicon wafer and the supporting waveguide; thus, enhancing its power handling capability.

I INTRODUCTION

During the past few years high power rf pulse compression systems have developed considerably. These systems provide a method for enhancing the peak power capability of high power rf sources. One important application is driving accelerator structures. In particular, future linear colliders, such as the proposed

[*] Also with Electrical Communications and Electronics Department, Cairo University, Giza, Egypt

NLC [2], require peak rf powers that can not be generated by the current state of the art microwave tubes[3].

The SLED Pulse compression system [4] was implemented to enhance the performance of the two mile accelerator structure at Stanford Linear Accelerator Center (SLAC). One drawback of SLED is that it produces an exponentially decaying pulse. To produce a flat pulse and to improve the efficiency, the Binary Pulse Compression (BPC) system [5] was invented. The BPC system has the advantage of 100% intrinsic efficiency and a flat output pulse. Also, if one accepts some efficiency degradation, it can be driven by a single power source [6]. However, The implementation of the BPC[7] requires a large assembly of over-moded waveguides, making it expensive and extremely large in size. The SLED II pulse compression system is a variation of SLED that gives a flat output pulse[8]. The SLED II intrinsic efficiency is higher than SLED [9], but not as good as BPC. However, from the compactness point of view SLED II is far superior to BPC. In this paper we present a variation on SLED II that will enhance its intrinsic efficiency without increasing its physical size.

The SLED II pulse compression system employs high Q resonant delay lines to store the energy during most of the duration of the incoming pulse. The round trip time of an rf signal through one of the delay lines determines the length of the compressed pulse. To discharge the lines, the phase of the incoming pulse is reversed 180° so that the reflected signal from the inputs of the lines and the emitted field from the lines add constructively thus, forming the compressed, high power, pulse.

The SLED II system suffers from two types of losses that reduce its intrinsic efficiency. During the charging phase some of the energy is reflected at the delay line entrance, and never gets into the lines. Also, after the phase is reversed the energy inside the lines is not discharged completely in one compressed pulse time period. These two effects make the intrinsic efficiency of SLED II deteriorate very fast at large compression ratios[8]. To reduce the amount of energy left-over after the output pulse is finished one can increase the coupling of the line just before the start of the output pulse. This will allow more energy to get out of the storage line during the compressed pulse time period. To reduce the losses due to reflections during the charging of the delay lines, one can optimize the constant line coupling for maximum energy storage.

To change the coupling coefficient of the storage lines, we designed a fast high power microwave switch. It is based on Bulk effects in semiconductors [10]. The device is optically controlled. We show a design that can handle, in principle, multi-megawatt microwave signals. Past experience with high power microwave ceramic windows [11] suggests that we will have a higher peak power handling capability by avoiding any electrical field at the interface between the

semiconductor wafer and the walls of the supporting waveguide. Hence, we designed the switch to operate at the TE_{01} mode in a circular waveguide.

In section II, we introduce a theory for optimizing the efficiency of the pulse compression system using one change in line coupling just before the discharging phase. In section III we analyze a symmetric 3-port device. We explore the ability of controlling the coupling between two of the ports by actively changing the termination of the third port. We derive general expressions for, power losses and peak electric field in that third arm, which we shall call the active arm. In section IV we present the design of the optical switch. In section V we describe the implementation of the system and present some experimental results.

II ACTIVE PULSE COMPRESSION USING SINGLE EVENT SWITCHED RESONANT DELAY LINES

The theory of active pulse compression with several time events is detailed in [1]. Here, we describe the special case of a *single event* switched pulse compression system.

A. Passive Pulse Compression

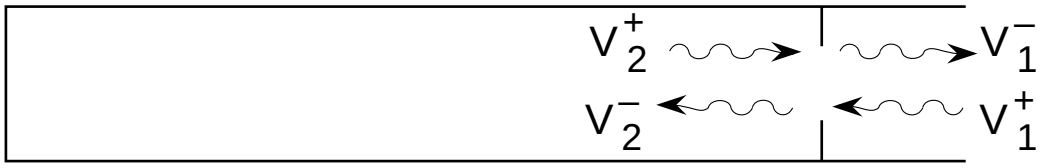

1–95 7874A1

Figure 1. Resonant delay line.

Consider the waveguide delay line with a coupling iris shown in Figure 1. The *lossless* scattering matrix representing the iris is unitary. At a certain reference plane the matrix takes the following form :

$$\underline{\underline{S}} = \begin{pmatrix} -R_0 & -j(1-R_0^2)^{1/2} \\ -j(1-R_0^2)^{1/2} & -R_0 \end{pmatrix}. \tag{1}$$

In writing Eq. (1) we assumed a symmetrical structure for the iris two port network. The forward and reflected fields around the iris are related as follows:

$$V_1^- = -R_0 V_1^+ - j(1-R_0^2)^{1/2} V_2^+ , \tag{2}$$

$$V_2^- = -j(1-R_0^2)^{1/2} V_1^+ - R_0 V_2^+ . \tag{3}$$

With the exception of some phase change, the incoming signal V_2^+ at time instant t is the same as the outgoing signal V_2^- at time instant $t-\tau$; where τ is obviously the round trip delay through the line; i.e.

$$V_2^+(t) = V_2^-(t-\tau)e^{-j2l\beta}; \tag{4}$$

where β is the wave propagation constant within the delay line, and l is the length of the line. Substituting from Eq. (4) into Eq. (3) we get

$$V_2^-(t) = -j(1-R_0^2)^{1/2} V_1^+(t) - R_0 V_2^-(t-\tau)e^{-j2l\beta} . \tag{5}$$

During the charging phase we assume a constant input, i.e., $V_1^+(t) = Vin$ which equals a constant value. We, also, assume that all the voltages are equal to zero at time $t < 0$. Hence, substituting the solution of the difference equation (5) into Eq. (4) leads us to write

$$V_2^+(i) = -j\frac{1-(-R_0 e^{-j2\beta l})^i}{1+R_0 e^{-j2\beta l}}(1-R_0^2)^{1/2} e^{-j2\beta l} Vin . \tag{6}$$

In Eq. (6) $V_2^+(i)$ means the incoming wave in the time interval $i\tau \le t < (i+1)\tau$ and $i \ge 0$. Substituting from Eq. (6) into Eq. (2) we get

$$V_1^-(i) = -Vin\left[R_0 + (1-R_0^2)\frac{1-(-R_0 e^{-j2\beta l})^i}{1+R_0 e^{-j2\beta l}} e^{-j2\beta l} \right]. \tag{7}$$

If the delay line has small losses (β has a small imaginary part), at resonance the term

$$e^{-j2\beta l} = -p . \tag{8}$$

where p is a positive real number close to 1. Eq. (7) becomes

$$V_1^-(i) = -Vin\left[R_0 - (1-R_0^2)\frac{1-(R_0 p)^i}{1-R_0 p} p \right]. \tag{9}$$

After the energy has been stored in the line one may dump part of the energy in a time interval τ by flipping the phase of the incoming signal just after a time interval $(n-1)\tau$, .i.e.,

$$V_1^+(t)=\begin{cases} Vin & 0\le t<(n-1)\tau \\ -Vin & (n-1)\tau\le t<n\tau \\ 0 & otherwise. \end{cases} \tag{10}$$

The output pulse level during the time interval $(n-1)\tau \le t < n\tau$ can be calculated from Eq. (2) with the aid of Eq.(6). The result is

$$V_{out}=V_1^-(n-1)=Vin\left[R_0+(1-R_0^2)\frac{1-(R_0p)^{n-1}}{1-R_0p}p\right]. \tag{11}$$

Indeed, this is the essence of the SLED II pulse compression system.

To illustrate the sources of inefficiency of the SLED II system we plot the output $V_1^-(t)$ vs. time (Figure 2). In this graph n=8, and the value R_0 =0.733. This value maximizes Eq. (11). Initially, the line is empty and a large portion of the incident power is reflected. Gradually, the reflected power decreases as the line is filled with energy. The reflected power starts to increase again as the line becomes almost fully charged. After the phase of the incoming signal is reversed, the compressed pulse appears. However, not all the energy of the line is dumped out; some of it is still in the line. This energy leaks out gradually after the compressed pulse.

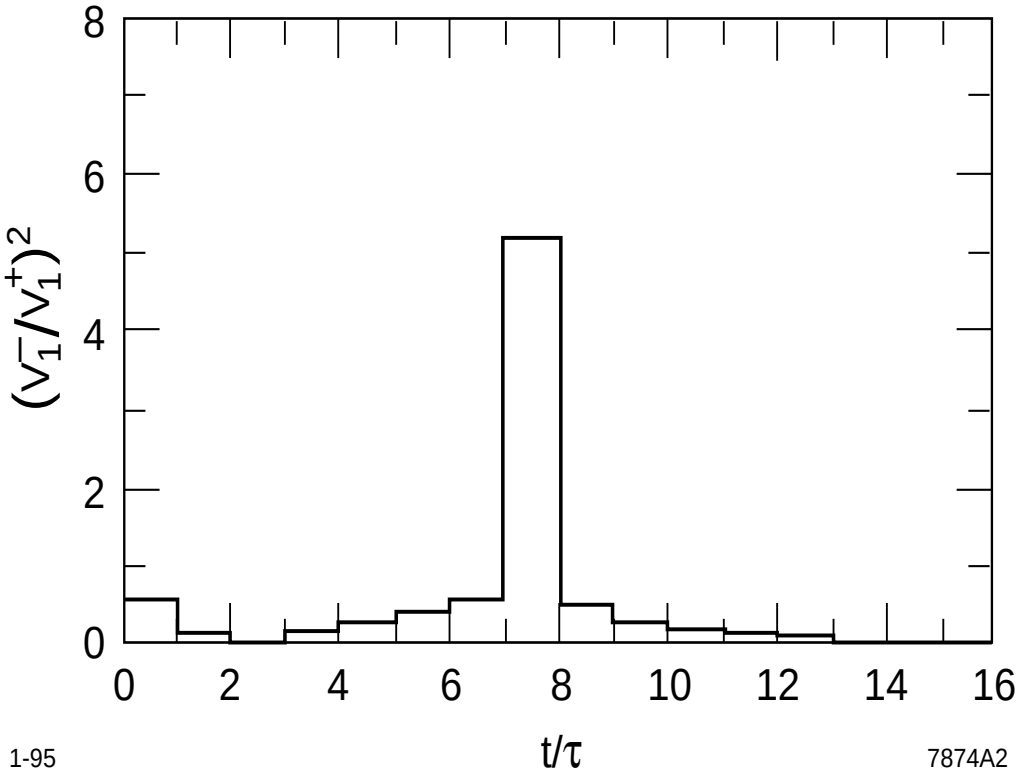

Figure 2. SLED II output for a compression ratio of 8.

The maximum power gain of SLED II is limited. Using Eq. (11), the power gain as $n \to \infty$ is,

$$\left(\frac{V_{out}}{Vin}\right)^2\Bigg|_{n\to\infty} = \left[R_0 + (1-R_0^2)\frac{p}{1-R_0 p}\right]^2; \tag{12}$$

which has a maximum value of

$$Maximum\,Power\,Gain = \frac{17}{p^2} - 8 - \frac{12\sqrt{2(1-p^2)}}{p^2} \tag{13}$$

at

$$R_0 = \frac{1}{p} - \frac{\sqrt{8(1-p^2)}}{4p}. \tag{14}$$

Clearly the maximum power gain is limited to 9 as $p \to 1$. Furthermore, this maximum is greatly affected by the losses in the delay line; for example, the gain is limited to 7.46 if the line has a 1% round trip power losses.

B. Active Switching During Charging Time

During the charging period the power reflected from the line reaches a maximum during the first time interval τ. Hence, one could initially make the iris reflection coefficient zero. After the first time interval τ we could switch the iris so that the reflection coefficient has a value R_0. Under these conditions, the difference equation (5) can be solved with the initial condition

$$V_2^-(0) = -jVin. \tag{15}$$

Solving Eq. (5) and substituting into (4) we get

$$V_2^+(i) = -je^{-j2\beta l}\left[\frac{1-(-R_0e^{-j2\beta l})^{i-1}}{1+R_0e^{-j2\beta l}}(1-R_0^2)^{1/2} + (-R_0e^{-j2\beta l})^{i-1}\right]Vin. \tag{16}$$

Assuming a resonant line and flipping the phase according to Eq. (10) the output pulse expression takes the following form

$$Vout = \left[\frac{1-(R_0p)^{n-2}}{1-R_0p}(1-R_0^2)p + (1-R_0^2)^{1/2}\,p(R_0p)^{n-2} + R_0\right]Vin. \tag{17}$$

Again the choice of the value of R_0 is such that *Vout* is maximized.

C. Active Switching during delay line Discharge

Case 1: Discharging After The Last Time Bin

To discharge the line, one can keep the input signal at a constant level during the time interval $0 \le t < n\tau$ but switching the iris reflection coefficient to zero so that all the energy stored in the line is dumped out. In this case

$$Vout = \frac{1-(R_0p)^n}{1-R_0p}(1-R_0^2)^{1/2}\,pVin. \tag{18}$$

Case 2: Switching Just Before The Last Time Bin

To reduce the burden on the switch one can reverse the phase together with changing the iris reflection coefficient. In this case all the energy can still be dumped out of the line, but the iris reflection coefficient need not be reduced completely to zero. During the discharge interval the new iris S matrix parameters can be written in the following form:

$$\underline{\underline{S}} = \begin{pmatrix} -\cos(\theta) & -j\sin(\theta) \\ -j\sin(\theta) & -\cos(\theta) \end{pmatrix}. \tag{19}$$

Applying Eq. (19) into Eq. (3) while setting $V_2^- = 0$ leads us to write

$$R_d = \cos\left[\tan^{-1}\left(\frac{1-(R_0 p)^{n-1}}{1-R_0 p}(1-R_0^2)^{1/2} p\right)\right]. \tag{20}$$

This new reflection coefficient is greater than zero and the switch need only change the iris between R_0 and R_d. Applying Eq. (16) into Eq. (2), the output reduces to

$$Vout = R_d\left[1+\left(\frac{1-(R_0 p)^{n-1}}{1-R_0 p}\right)^2 (1-R_0^2) p^2\right] Vin\,. \tag{21}$$

The compressed pulse takes place in the interval $(n-1)\tau \le t < n\tau$. The optimum value of R_0 is such that it fills the system with maximum possible amount of energy in the time interval $(n-1)\tau$ instead of $n\tau$ in the previous case. Unlike the previous case the incident power during this interval will not coupled to the line nor suffer from a round trip loss. Therefore, the system, in this case, has a higher efficiency. Figure 3. shows an example of this case.

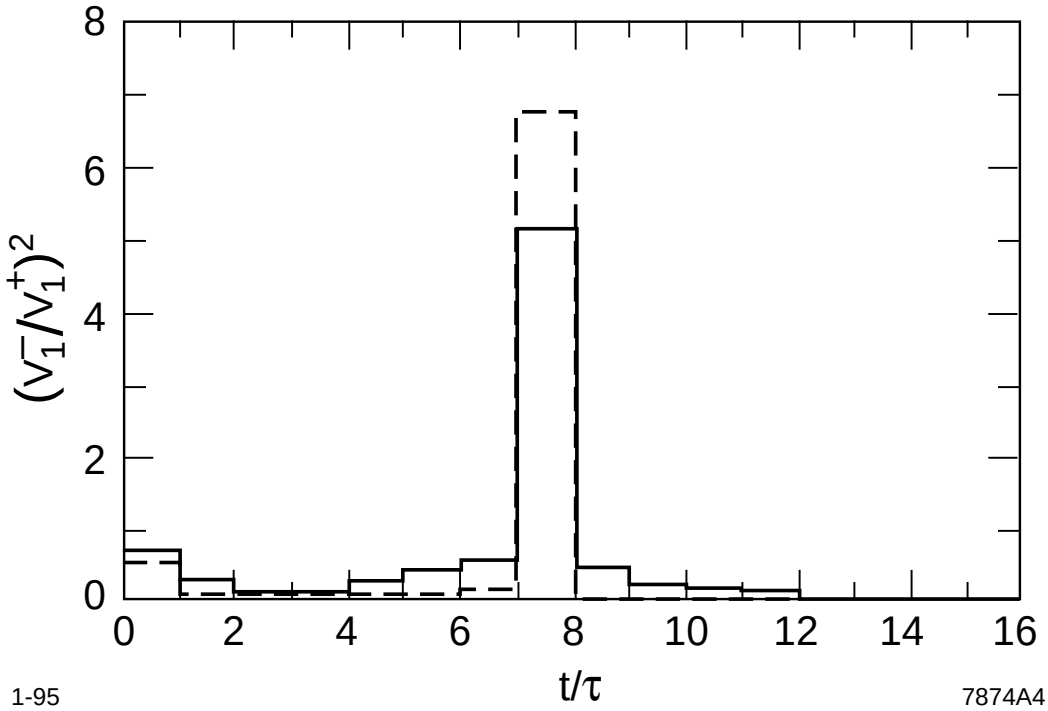

Figure 3. Comparison between SLED II output and a one time switched resonant delay line for a compression ration of 8. The line is switched just before the last time bin. Thick curve represent switched line, and thin curve represent SLED II.

For both cases of discharging by active switching, the maximum power is

$$Maximum\,Power\,Gain = \frac{p^2}{1-p^2}; \tag{22}$$

which occurs at

$$R_0 = p\,. \tag{23}$$

Unlike the passive system, the maximum power gain has no intrinsic limit. It is only limited by the amount of losses in the storage line. In this case the gain can be much higher than 9, which is the limit of the passive system.

D. Effect of losses

As the compression ratio increases, the stored energy spends more time in the storage lines resulting in a reduction in efficiency due to the finite quality factor of the lines. Figure 4 shows the effect of losses for different compression ratios. The round trip line loss plus reflection losses at the end of the line plus reflection losses at the active iris is defined as

$$Round\ \ Trip\ \ Power\ \ Loss = 1 - p^2 . \tag{24}$$

In Figure 4. for a given C_r the method used to switch the iris is the optimum one for this particular C_r .

At the last time bin the phase of the incoming signal is flipped and the coupling iris reflection coefficient changes from R_0 to R_d. The table shows, also, the optimum coupling iris reflection coefficient in both cases. As the compression ratio, C_r, increases the efficiency of SLED II decreases dramatically; while that of the active system remains above 81%.

E. Comparison

Table 1. compares the different types of pulse compression systems. It also gives the optimum system parameters for each compression ratio C_r ; here C_r is defined as the total time interval divided by the duration of the compressed pulse, i.e., n . The efficiency of the system η, is defined as the energy in the compressed pulse divided by the total incident energy, namely

$$\eta = \frac{1}{C_r}\left(\frac{Vout}{Vin}\right)^2 . \tag{25}$$

In these calculations we assume a lossless system, i.e., $p = 1$.

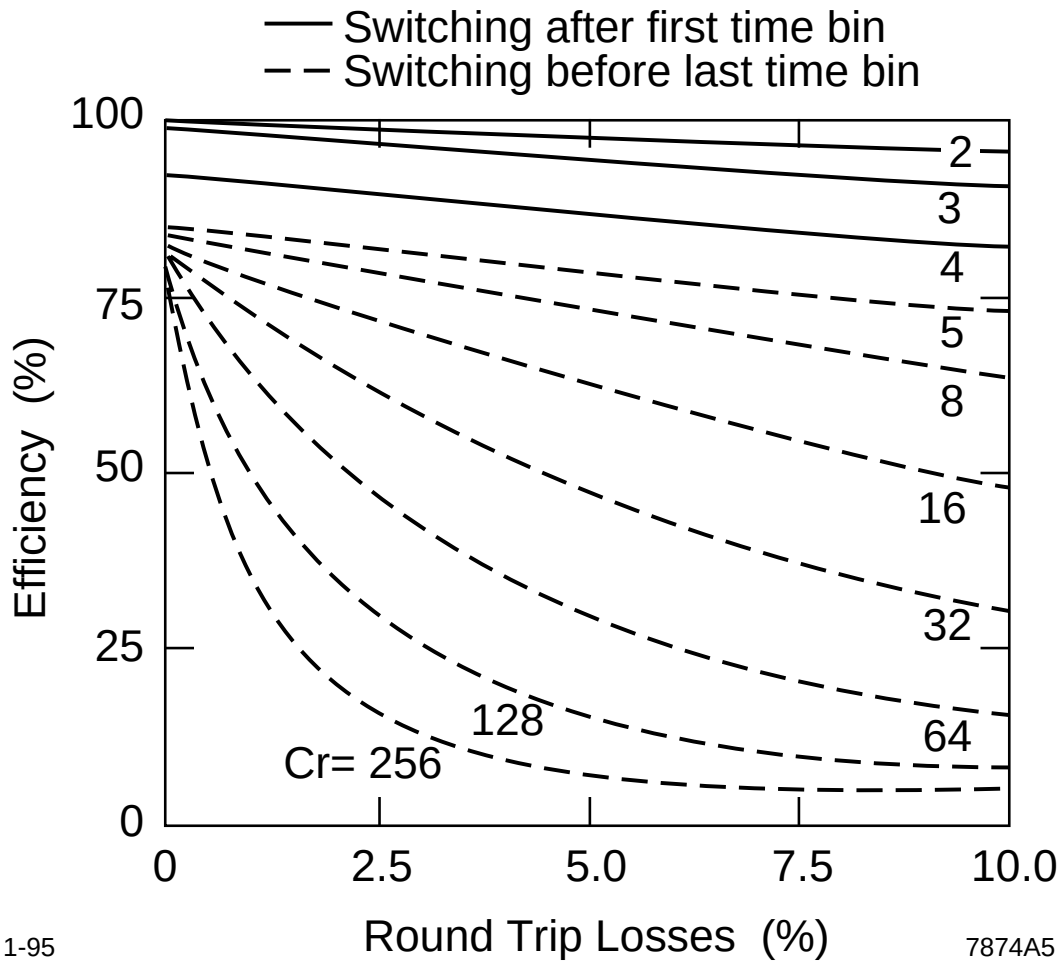

Figure 4. Effect of line and switching iris losses on compression efficiency for a one time switched resonant delay line.

					Discharging By Active Switching				
C_r	SLED II		Switching During Charging Time		Discharging After The Last Time Bin.		Discharging Just Before The Last Time Bin		
	η (%)	Opt. R_0	η (%)	Opt. R_0	η (%)	Opt. R_0	η (%)	Opt. R_0	R_d
2	78.1	0.5	100	0.707	84.4	0.5	100	0.0	0.707
3	88.7	0.548	98.9	0.631	82.7	0.646	89.6	0.5	0.610
4	86.0	0.607	92.6	0.658	82.1	0.725	87.0	0.646	0.536
5	80.4	0.651	85.1	0.688	81.9	0.775	85.7	0.725	0.483
6	74.6	0.685	78.1	0.714	81.8	0.809	84.9	0.775	0.443
8	64.4	0.733	66.5	0.754	81.6	0.854	84.0	0.835	0.386
10	56.2	0.767	57.7	0.783	81.6	0.882	83.4	0.869	0.346
12	49.9	0.792	50.9	0.805	81.5	0.900	83.1	0.892	0.317
16	40.6	0.828	41.2	0.837	81.5	0.924	82.7	0.920	0.275
24	29.6	0.869	29.8	0.875	81.5	0.949	82.2	0.947	0.225
32	23.3	0.893	23.4	0.897	81.5	0.961	82.0	0.960	0.195
64	12.6	0.936	12.7	0.938	81.5	0.981	81.7	0.980	0.138
128	6.6	0.962	6.6	0.963	81.5	0.990	81.6	0.990	0.099
256	3.4	0.978	3.4	0.979	81.5	0.995	81.5	0.995	0.069

Table 1. Comparison between different methods of single event switching pulse compression systems.

At small values of C_r, switching the iris just after the first time bin is the most efficient solution. When $C_r \geq 5$, switching the iris just before the last time

bin while reversing the phase by 180° is more efficient. At high compression ratios, the last time bin does not contribute much. Hence, switching the iris after the last time bin is almost equivalent to switching it just before the last time bin. For applications that require one pulse compression system or several pulse compression system with no phase synchronization switching after the last time bin may be advantageous because it can use an oscillator as the primary rf source instead of an amplifier or a phase locked oscillator.

In general, switching the line just before the last time bin is the most advantageous technique. For reasonably high compression ratios the change in the iris reflection coefficient is relatively small. This simplifies the high power implementation of the active iris. Also, the losses in the delay line make the efficiency of the system deteriorates with higher compression ratios. Clearly, the active system is advantageous at high compression ratios. However, it soon loses its advantage because of delay line losses. Between the compression ratios of 6 and 32 the active system has a significant advantage over the passive one. At the same time the delay line losses does not reduce its efficiency in a significant way.

III MICROWAVE CONTROL USING A SYMMETRIC THREE PORT NETWORK

Consider the three port device shown in Figure 5. The device is composed of a basic *lossless* three port device with two similar ports, namely, port 1 and port 2. The third port is terminated so that all the scattered power from that port is completely reflected. However, the phase of the reflected signal from the third port can be changed actively. For any lossless and reciprocal 3-port network the scattering matrix is unitary and symmetric. By imposing these two conditions on the scattering matrix $\underline{\underline{S}}$ of our device and at the same time taking into account the symmetry between port one and port two, at some reference planes, one can write:

$$\underline{\underline{S}} = \begin{pmatrix} \frac{e^{j\phi} - \cos\theta}{2} & \frac{-e^{j\phi} - \cos\theta}{2} & \frac{\sin\theta}{\sqrt{2}} \\ \frac{-e^{j\phi} - \cos\theta}{2} & \frac{e^{j\phi} - \cos\theta}{2} & \frac{\sin\theta}{\sqrt{2}} \\ \frac{\sin\theta}{\sqrt{2}} & \frac{\sin\theta}{\sqrt{2}} & \cos\theta \end{pmatrix}; \qquad (26)$$

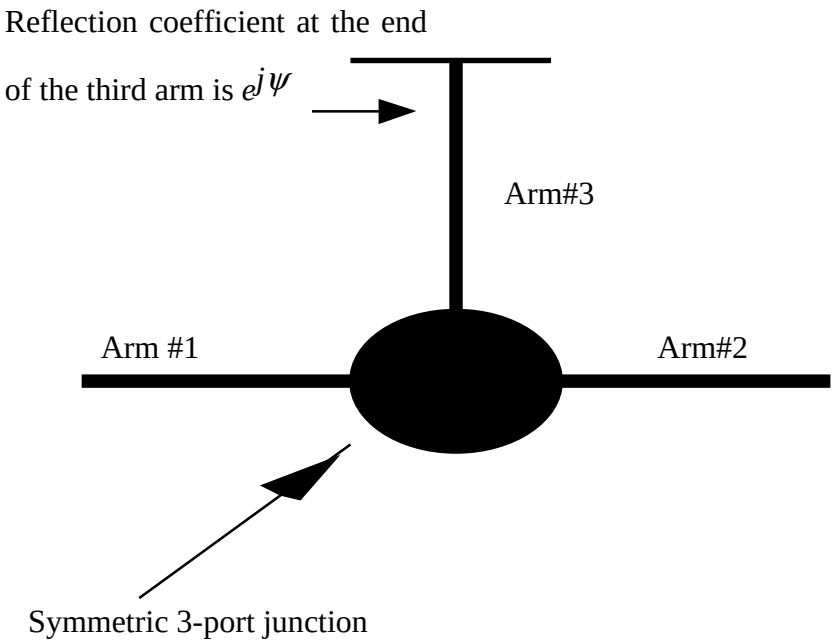

Figure 5. A symmetric three port network. The third arm is terminated with a short circuit.

Indeed, with the proper choice of the reference planes, this expression is quite general for any symetric three port network. The scattering matrix properties are determined completely with only two parameters: θ and ϕ.The scattered rf signals $\underline{V}^-$ are related to the incident rf signals $\underline{V}^+$ by

$$\underline{V}^- = \underline{\underline{S}}\underline{V}^+ ; \tag{27}$$

where $V_i^{\pm}$ represents the incident/reflected rf signal from the *i*th port. We terminate the third port so that all the scattered power from that port is completely reflected; i.e.,

$$V_3^+ = V_3^- e^{j\psi} . \tag{28}$$

The resultant, symmetric, two port network, then, has the following scattering matrix parameters:

$$S_{11} = S_{22} = \frac{\left(e^{j\psi} + e^{j\phi}\right) - \left(1 + e^{j(\phi+\psi)}\right)\cos\theta}{2\left(1 - \cos\theta\, e^{j\psi}\right)}, \tag{29}$$

$$S_{12} = S_{21} = \frac{\left(e^{j\psi} - e^{j\phi}\right) - \left(1 - e^{j(\phi+\psi)}\right)\cos\theta}{2\left(1 - \cos\theta\, e^{j\psi}\right)}. \tag{30}$$

By changing the angle ψ of the third port terminator, the coupling between the first and the second ports can vary from 0 to 1.

The signal level at the third arm is, then, given by:

$$\left|V_3^+\right|^2 = \left|V_3^-\right|^2 = \frac{\sin^2\theta}{3 - 4\cos\theta\cos\psi + \cos 2\theta}\left|V_1^+ + V_2^+\right|^2. \tag{31}$$

This signal level is independent of the parameter ϕ. and has a maximum or a minimum value at ψ =0 or π.

IV THE OPTICAL SWITCH

A. Device Physics

To actively change the angle of the reflection coefficient at the third port we place a piece of semiconductor material in the third arm. An external stimulus such as a laser light can induce an electron-hole plasma layer at the surface of the semiconductor, thus changing its dielectric constant. Therefore, the propagation constant of rf signals through the active arm changes; and consequently the coupling between the other two ports also changes.

For the pulse compression system application associated with the NLC [2], for which we choose a compression ratio of 8, it is required to change the reflection coefficient at the first arm between two fixed values. The device should remain in one state for approximately 1.75μsec, and in the other state for 250 nsec. Since silicon has a carrier lifetime that can extend from 1 μsec to 1 msec it seems like a natural choice for this application. One can excite the plasma layer with a very short pulse from the external stimulus (~5nsec) and the device will stay in its new status longer than the duration of the rf signal. Since repetition rate for this pulse compression system is 180 pulse/sec there is sufficient time between pulses for the switch to completely recover.

To be useful, this switch needs to have a very small amount of losses. Following classical arguments[12], one can show that the dielectric constant of a semiconductor material is

$$\varepsilon = \varepsilon_0 \varepsilon_r \left(1 - \sum_i \frac{X_i}{1 - jZ_i} \right); \tag{32}$$

where

$$X_i = \frac{N_i e^2}{\varepsilon_0 \varepsilon_r m_i^* \omega^2} , \tag{33}$$

$$Z_i = \frac{\nu_i}{\omega}, \tag{34}$$

where ω is the radial frequency of the rf signal, m_i^* is the effective mass of carrier i (electron, light hole and heavy hole), N_i is carrier density, e is the electron charge, and ν_i is the collision frequency. This latter quantity is related to the measured values of the dc mobility μ_i[12] as follows:

$$\frac{1}{\nu_i} = \frac{\mu_i m_i^*}{e} . \tag{35}$$

Comparison between estimates of ν_i for silicon at 11.424 GHz, the operating frequency of the NLC, shows that $Z_i >> 1$. Hence, one can show that the dielectric constant is given by the classical relation

$$\varepsilon = \varepsilon_0 \varepsilon_r \left(1 - j \frac{\sigma}{\omega \varepsilon_0 \varepsilon_r} \right); \tag{36}$$

where

$$\sigma = e \sum_i \mu_i N_i , \tag{37}$$

which is the conductivity of the semiconductor.

To minimize the losses in the off state, i.e., when there is no plasma excited, we need to have a very pure semiconductor material such that the intrinsic carrier density is very small. In the On state, i.e., when the plasma layer

is excited, the carrier density should be large enough so that the semiconductor acts like a good conductor and thus minimizing the losses.

At a carrier density of $10^{19}/cm^3$, silicon has a conductivity of ~$3.3x10^3$ mho/cm. This is two orders of magnitude smaller than that of copper. However, it is high enough to make an effective reflector. The skin depth of an rf signal at the NLC frequency at this conductivity level is ~8μm. In choosing the laser wavelength to produce the photo-induced carriers, light penetration depth should be comparable to this skin depth.

B. Design Methodology

While charging the delay line with rf energy, the reflection coefficient of the coupling iris is R_0, as given in table 1 for different compression ratios. Hence, the first design equation is

$$|S_{11}|^2 = R_0^2 = \frac{\left(\cos(\frac{\phi+\psi_c}{2}-\theta)+\cos(\frac{\phi+\psi_c}{2}+\theta)-2\cos(\frac{\phi-\psi_c}{2})\right)^2}{4-8\cos(\psi_c)\cos(\theta)+4\cos^2(\theta)}, \quad (38)$$

which follows immediately from Eq. (29). The angle ψ_c is the angle of the reflection coefficient of the third arm during the charging time. During the charging time, the charging signal is constant and is equal to Vin. Hence, using Eq. (31), and (6) one can write an expression for the field level in control arm (the third arm)

$$\left|V_3^+\right| = \left|V_3^-\right| = \frac{\sin\theta}{\left(3-4\cos\theta\cos\psi_c+\cos 2\theta\right)^{1/2}}\left| j\frac{1-(R_0 p)^{C_r-2}}{1-R_0 p}(1-R_0^2)^{1/2}p+1\right| Vin \quad (39)$$

During the charging time, we choose the angle $\psi_c = \pi$. Eq. (38) then becomes

$$R_0^2 = \sin^2\frac{\phi}{2}. \quad (40)$$

That determines the angle ϕ completely. Eq. (39) becomes:

$$\left|V_3^+\right| = \left|V_3^-\right| = \frac{1}{\sqrt{2}}\tan\frac{\theta}{2}\left| j\frac{1-(R_0 p)^{C_r-2}}{1-R_0 p}(1-R_0^2)^{1/2}p+1\right| Vin. \quad (41)$$

During the discharging time the angle ψ would change from π to the new value ψ_d, Hence the active layer, i.e. silicon wafer will be placed at a point which has a reduced electric field by a factor of $\sin\psi_d$. One then, writes an expression for the maximum field seen by the silicon wafer during the charging time:

$$E_{\max} = 2\left|\tan\frac{\theta}{2}\cos\frac{\psi_d}{2}\right| j\frac{1-(R_0 p)^{C_r-2}}{1-R_0 p}(1-R_0^2)^{1/2} p+1\left|\left(\frac{P_{in}Z_3}{A_3 G_3}\right)^{1/2}\right|; \qquad (42)$$

where P_{in} is the constant level input power, Z_3 is the wave impedance of the mode excited in the waveguide that forms the third arm, A_3 is the cross sectional area of that guide, and G_3 is a geometrical factors that depends on the mode and the waveguide shape of the third arm. The angle ψ_d should satisfy:

$$\left|S_{11}\right|^2 = R_d^2 = \frac{\left(\cos(\frac{\phi+\psi_d}{2}-\theta)+\cos(\frac{\phi+\psi_d}{2}+\theta)-2\cos(\frac{\phi-\psi_d}{2})\right)^2}{4-8\cos(\psi_d)\cos(\theta)+4\cos^2(\theta)}; \qquad (43)$$

where R_d is given by Eq. (20), and its numerical values is tabulated in Table 1. Finally at the discharging time the signal level at the third arm is given by:

$$\left|V_3^+\right| = \left|V_3^-\right| = \frac{\sin\theta}{\left(3-4\cos\theta\cos\psi_d+\cos 2\theta\right)^{1/2}}\left| j\frac{1-(R_0 p)^{C_r-1}}{1-R_0 p}(1-R_0^2)^{1/2} p-1\right| Vin, \qquad (44)$$

which leads us to write an expression for the amount of losses in the silicon wafer during the discharging time, P_l:

$$P_l = \left(\frac{2\sin\theta}{\left(3-4\cos\theta\cos\psi_d+\cos 2\theta\right)^{1/2}}\left| j\frac{1-(R_0 p)^{C_r-1}}{1-R_0 p}(1-R_0^2)^{1/2} p-1\right|\right)^2 \frac{R_s}{Z_3} P_{in}; \qquad (45)$$

where R_s is the surface resistance and is given by

$$R_s = \left(\frac{\omega\mu_0}{2\sigma}\right)^{1/2}. \qquad (46)$$

The value of the conductivity σ is given by Eq. (37). Clearly one wants to use as much laser power as possible to maximize σ.

Equations (40), (42), (43), and (45) are the design equations. The goal of the design is to reduce the electric field below 100 kV/cm during the charging time; which is the estimated breakdown field for a silicon wafer with a relatively large size. At the same time one should keep the losses in the silicon wafer below a certain limit so that the temperature of the wafer does not rise above a certain temperature, say 70 C°. If this temperature is exceeded, a risk of thermal runaway exists; as the silicon wafer gets hotter the losses, during discharging time increase,

causing the temperature rise further until the silicon wafer becomes conductive because of thermal effects alone.

C. Switching Time

The calculations of the switching time of this system is governed by the filling time of the third arm. To calculate this time accurately one must know how all the system components behave with frequency. This is beyond the scope of the current analysis. However, one can have a conservative estimate for that time by considering only the third arm at resonance. If this arm has an approximate length of one-half wavelength, and couples to the outside world with an iris that has a reflection coefficient equals to cosθ (S_{33}=cosθ; see Eq. (25)) the filling time T_f Then can readily shown to be

$$T_f = \frac{-\left(1-\left(\frac{f_c}{f}\right)\right)^{-1/2}}{f\,\ln(\cos\theta)}; \qquad (47)$$

where f is the operating frequency. This equation assumes that the third port is at resonance, however, in the real operation of the switch the third arm is never brought to resonance. Hence, the expression puts an upper limit on the switching time.

D. A Design Example

The power required to be generated from an rf station in the NLC Test Accelerator [2] is 400 MW at a pulse width of 250 nS, at 11.424 GHz. This can be produced using the proposed 75 MW Klystrons [14] while compressing the output of these klystrons with a compression ratio of 8 and assuming a compression efficiency of 75%. To compress the rf signal efficiently by a factor of 8, the magnitude of the reflection coefficient of an iris needs to change between 0.835 and 0.386. We choose to operate the active arm at the TE_{01} mode of a circular waveguide. We choose this mode of operation because it has no normal field near the walls. Hence, one need not worry about the details of high field operation at the interface between the silicon wafer and the waveguide walls[11,15]. The geometrical factor G_3 , which appears in Eq. (42) equals 0.479 for that mode. Then, using Eq. (40) the angle ϕ=113.23°. We choose the radius of the third arm to be 2.78 cm. This radius will allow the TE_{01} mode to propagate and will cutoff the TE_{02} mode. We then choose the angle θ=122.4°. This will make the rise time of the switch less than 2 nS (Eq. (47)). To satisfy Eq. (43), the angle ψ_d = 202.97°. The field amplitude in the third arm during the charging time is estimated with the help of Eq. (42) to be 95.5 kV/cm. Finally, according to Eq. (45), the losses of the switch during the discharging time is 4.5%.

Figure 6. shows both the relative signal level in the third arm (Eq. (39); *Vin*=1) and reflection coefficient (S_{11} in Eq. (38)) as a function of the angle ψ for the switch parameters described above.

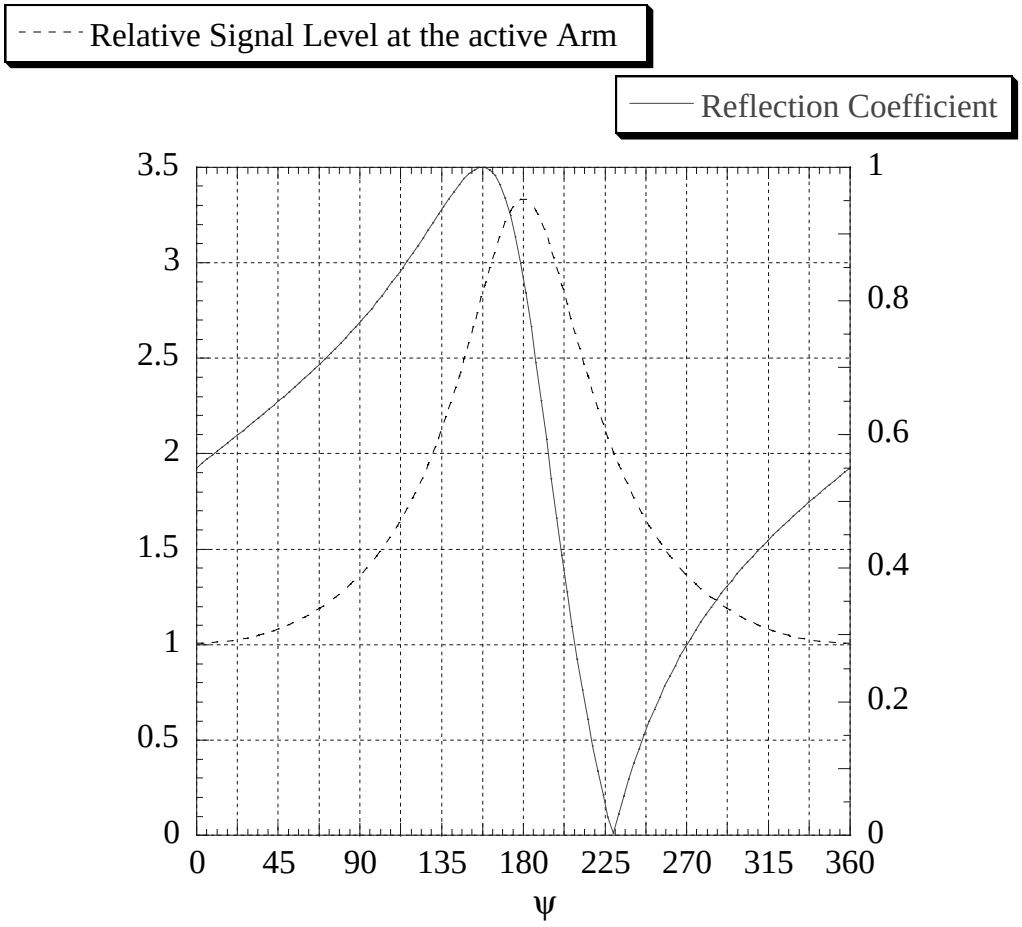

Figure 6. Reflection coefficient and the relative field level at the active arm vs. the angle ψ.

V PROOF OF PRINCIPLE EXPERIMENT

Figure 7 shows the schematic diagram of an active pulse compression experiment. A flower petal mode transducer[16] and a long circular waveguide act as the storage delay line. The waveguide is excited at the TE_{01} mode. A matched

magic tee, terminated with a short circuit at the E arm acts as the three port network. The TE_{01} mode switching arm (third arm) is connected to the H arm of the magic tee with a special side coupled mode converter[17]. The circular guide representing the third arm is terminated from one side by a short circuit plate and a 250 micron thick, 6000 ohm cm silicon wafer is placed between the shorting plate and the mode converter. From the other side of the mode converter, a TE_{01} choke act as a terminator for this circular guide, while allowing the laser light to reach the silicon wafer.

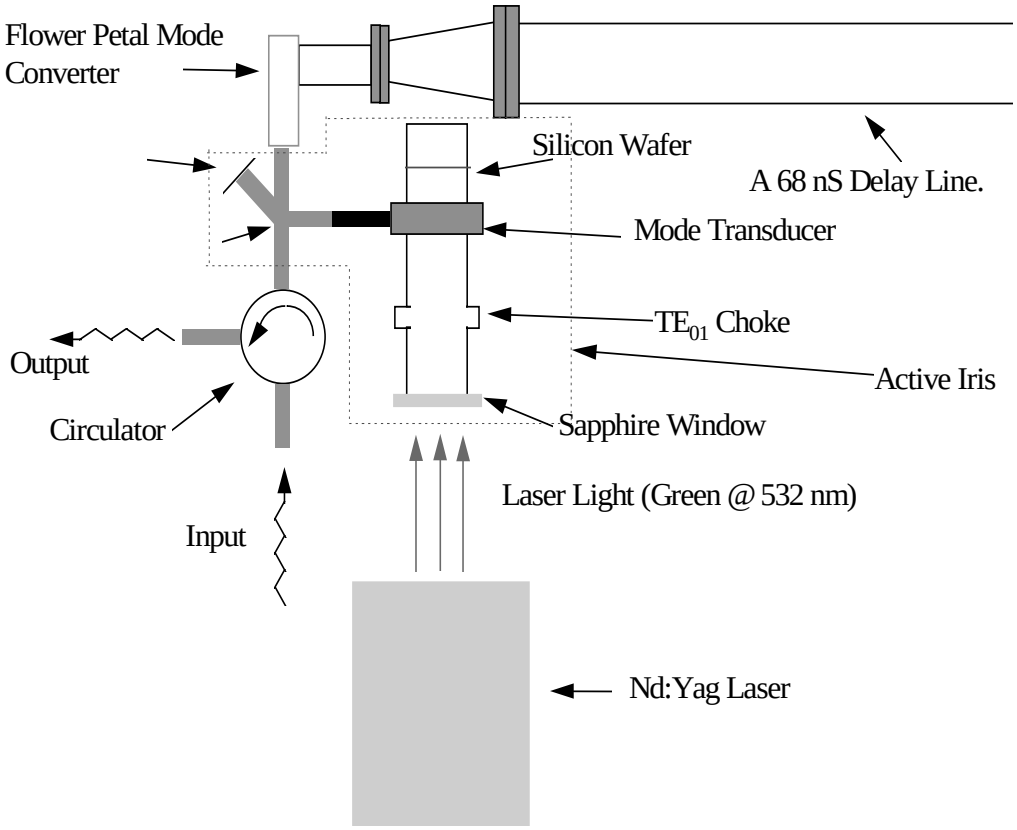

Figure 7. Schematic Diagram Of The Proof Of Principle Experiment.

We start our tuning of this switch by adjusting the shorting plate until the field in the circular arm reaches a maximum (See Figure 6). The field is observed by a small H probe placed near the choke during the cold test adjustments. This makes the angle $\psi_c = \pi$. Then the circular guide is connected to H arm of the magic tee. The movable short, which is connected to the E arm of the magic tee, is tuned until the reflection coefficient reaches R_0. Then, the laser is fired and the silicon wafer position is adjusted to get a reflection coefficient equals to R_d.

Figure 8 shows the output of this system at a compression ratio of 8. The system has a gain of 6. The passive pulse compression system, SLED II, has a theoretical gain of 5.1, and if one assumes similar losses in the delay line SLED II gain would drop to 4.2. Figure 9 shows the output of the system for a compression ratio of 32. The system has a gain of 11. SLED II has a theoretical gain of 7.4, and if one assume similar losses in the delay line SLED II gain would drop to ~5. Indeed, a gain of 11 is much more than the theoretical gain of any passive pulse compression system. These have a maximum gain of 9 as the compression ratio goes to infinity.

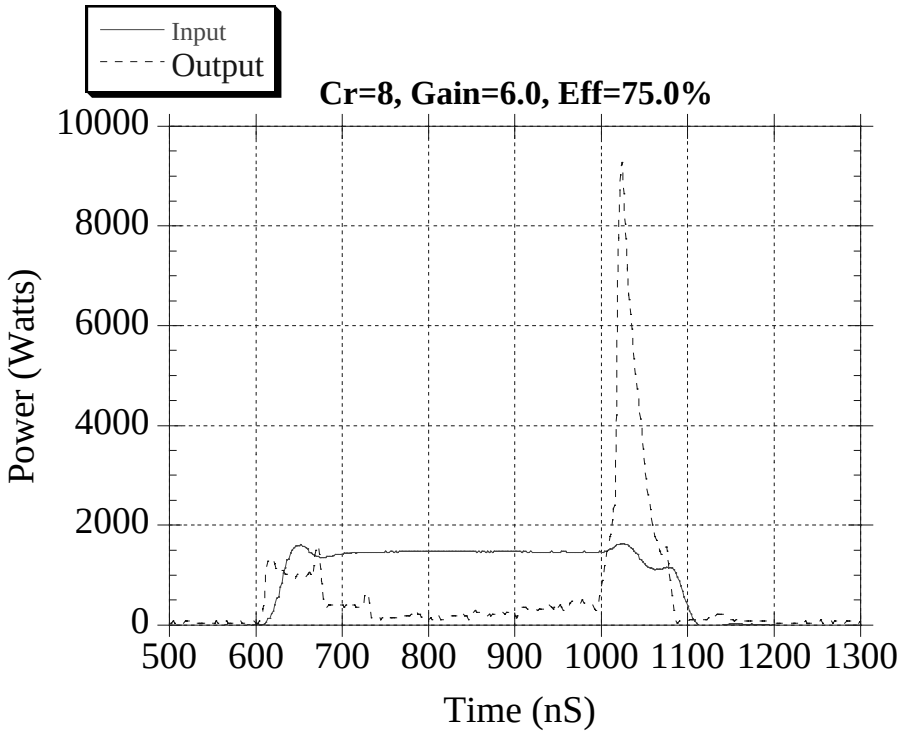

Figure 8. Experimental Output of the Active Pulse Compression System at a Compression Ratio of 8.

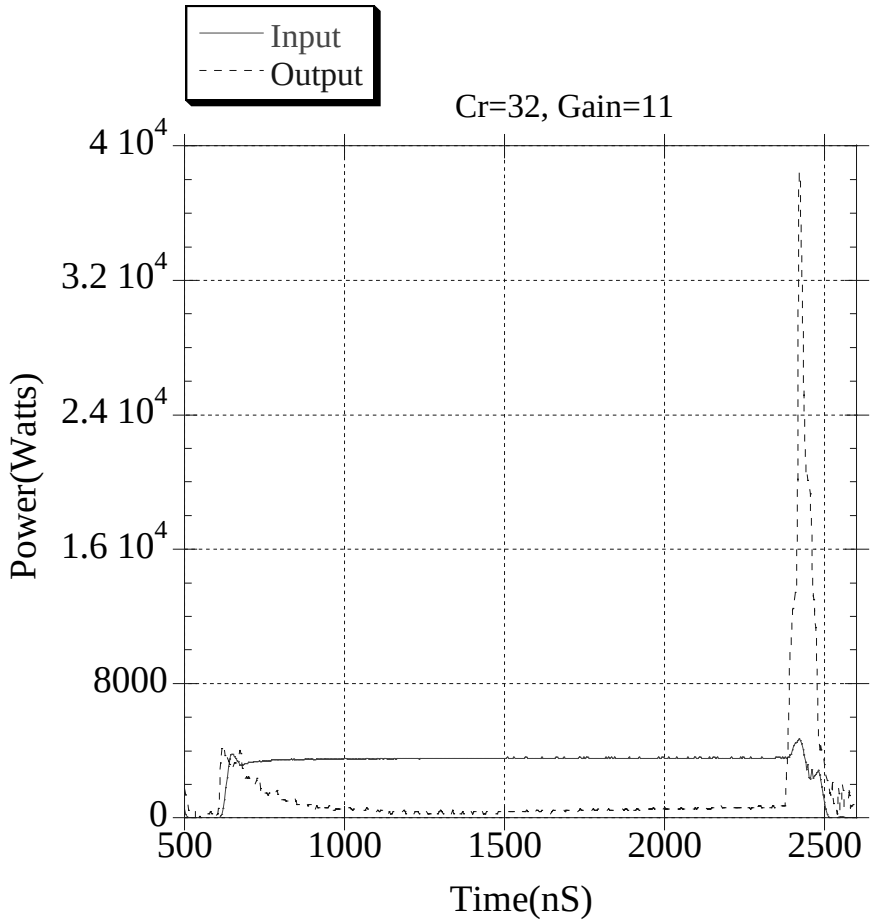

Figure 9. Experimental Output of the Active Pulse Compression System at a Compression Ratio of 32.

VI CONCLUSION

We have developed the theory for a single-time-switched resonant delay line pulse-compression system. We gave a design example for an active iris operating at the TE_{01} mode. We, finally, demonstrated the operation of such a switch. The system achieved a power gain of 11 at a compression ratio of 32. This

is more than the maximum theoretical gain of SLED II even as the compression ratio goes to infinity.

ACKNOWLEDGMENT

In 1988, Prof K. Zaki at the EE department of the University of Maryland had suggested to the first author that a devices based on bulk effect in semiconductors could be useful even at power levels as high as few tens of Megawatts. It was also suggested in 1988 by Prof Wayne Vernon at UCSD that bulk effects in semiconductors could develop a useful technique for rf pulse compression. The authors also appreciate the help of Terry G. Lee specially during the mechanical design phase of this device. This work is supported by the US Department of Energy under contract DE-AC03-76F00515.

REFERENCES

[1] S. G. Tantawi, et. al, "Active RF Pulse Compression Using Switched Resonant Delay Lines," Nuc. Inst. and Meth, A, Vol. 370 (1996), pp. 297-302; SLAC-PUB 6748.

[2] R. D. Ruth et. al., "The Next Linear Collider Test Accelerator," Proc. of the IEEE Particle Accelerator Conference, Washington DC, May 1993, p. 543.

[3] Proc. Conference on Pulsed RF Sources for Linear Colliders, Montauk, Long Island New York, October 2-7, 1994

[4] Z. D. Farkas et. al., "SLED: A Method of Doubling SLAC's Energy," Proc. of the 9th Int Conf. on High Energy Accelerators, 1976, p. 576.

[5] Z. D. Farkas, "Binary Peak Power Multiplier and its Application to Linear Accelerator Design," IEEE Trans. MTT-34, 1986.

[6] P. E. Latham, "The Use of a Single source to Drive a Binary Peak Power Multiplier," Linear Accelerator Conference, Williamsburg, Virginia, 1988, CEBAF-R-89-001, pp. 623-624.

[7] Z. D. Farkas, et . al., "Two-Klystron Binary Pulse Compression at SLAC," Proc. of the IEEE Particle Accelerator Conference, Washington DC, May 1993, p. 1208.

[8] P. B. Wilson, Z. D. Farkas, and R. D. Ruth, "SLED II: A New Method of RF Pulse Compression," Linear Accl. Conf., Albuquerque, NM, September 1990; SLAC-PUB-5330

[9] Z. D. Farkas, et. al., " Radio frequency pulse compression experiments at SLAC," SPIE's Symposium on High Power Lasers, Los Angeles, CA, January, 1991, also SLAC-PUB-5409.

[10] Lee, H. Chi, Editor, "Picosecond optoelectronic devices, " Academic Press Inc., Orlando, 1984.

[11] W.R. Fowkes,et. al. "Reduced Field TE_{01} X-Band Traveling Wave Window;" Proc. of the 16th IEEE Particle Accelerator Conference (PAC 95) and International Conference on High-energy Accelerators (IUPAP), Dallas, Texas, 1-5 May 1995; SLAC-PUB-6777, Mar 1995.

[12] Wait, J. R. "Electromagnetics and plasmas," Holt, Rinehart and Winston, Inc. New York, 1968

[13] SZE S. M. "Physics of semiconductor devices, "John Wiley & Sons, Inc., New York, 1969.

[14] D. Sprehn, et. Al. "PPM Focused X-Band Klystron Development At The Stanford Linear Accelerator Center," Proc. of the 3rd International Workshop on RF Pulsed Power Sources for Linear Colliders (RF 96), Hayama, Japan, 8-12 Apr 1996; SLAC-PUB-7231, Jul 1996

[15] S. G. Tantawi, et. al., "Design of a Multi-Megawatt X-Band Solid State Microwave Switch" Presented in the IEEE int. Conf. on Plasma Sci., Wisconsin, June, 1995.

[16] S. G. Tantawi et. al., "Numerical Design and Analysis of a Compact TE_{01} to TE_{11} Mode Transducer," Conference on computational Accelerator Physics, Los Alamos, NM, 1993, AIP Conference Proceedings 297, pp. 99-106.

[17] S. G. Tantawi et. al., "Compact TE_{10} (rectangular) to TE_{01} (Circular) Mode Converter for Over-Moded Waveguides," Patent disclosure to DOE April 30, 1996, DOE Patent Docket No. S-85,926 (RL-13545)